



Northern Arabian Sea Circulation- Autonomous Research (NASCar)

A RESEARCH INITIATIVE BASED ON AUTONOMOUS SENSORS

By Luca R. Centurioni, Verena Hormann, Lynne D. Talley, Isabella Arzeno, Lisa Beal, Michael Caruso, Patrick Conry, Rosalind Echols, Harindra J.S. Fernando, Sarah N. Giddings, Arnold Gordon, Hans Graber, Ramsey R. Harcourt, Steven R. Jayne, Tommy G. Jensen, Craig M. Lee, Pierre F.J. Lermusiaux, Pierre L'Hegaret, Andrew J. Lucas, Amala Mahadevan, Julie L. McClean, Geno Pawlak, Luc Rainville, Stephen C. Riser, Hyodae Seo, Andrey Y. Shcherbina, Eric Skyllingstad, Janet Sprintall, Bulusu Subrahmanyam, Eric Terrill, Robert E. Todd, Corinne Trott, Hugo N. Ulloa, and He Wang





ABSTRACT. The Arabian Sea circulation is forced by strong monsoonal winds and is characterized by vigorous seasonally reversing currents, extreme differences in sea surface salinity, localized substantial upwelling, and widespread submesoscale thermohaline structures. Its complicated sea surface temperature patterns are important for the onset and evolution of the Asian monsoon. This article describes a program that aims to elucidate the role of upper-ocean processes and atmospheric feedbacks in setting the sea surface temperature properties of the region. The wide range of spatial and temporal scales and the difficulty of accessing much of the region with ships due to piracy motivated a novel approach based on state-of-the-art autonomous ocean sensors and platforms. The extensive data set that is being collected, combined with numerical models and remote sensing data, confirms the role of planetary waves in the reversal of the Somali Current system. These data also document the fast response of the upper equatorial ocean to monsoon winds through changes in temperature and salinity and the connectivity of the surface currents across the northern Indian Ocean. New observations of thermohaline interleaving structures and mixing in setting the surface temperature properties of the northern Arabian Sea are also discussed.

INTRODUCTION

The Arabian Sea, in the northwestern Indian Ocean, plays a critical role in the Asian monsoon and associated precipitation over the Indian subcontinent. The seasonal monsoonal winds in turn force the seasonally varying circulation in the Arabian Sea (Schott and McCreary, 2001; Trott et al., 2017), but the feedback and adjustment processes between the ocean circulation, sea surface temperature (SST), and the atmosphere are not well understood.

The overarching goal of the Office of Naval Research (ONR)-funded Northern Arabian Sea Circulation-autonomous research (NASCar) initiative is to improve our understanding of the role that western tropical Indian Ocean processes, particularly those in the northern Arabian Sea, play in the onset and evolution of the Indian monsoon. The working hypothesis that connects the observational and modeling components of NASCar is that our limited knowledge of the local air-sea fluxes in the northwestern Indian Ocean limits the skills of models in correctly forecasting the onset and intraseasonal-to-interannual variability of the Asian monsoon, and that such fluxes are influenced by ocean mesoscale

and submesoscale dynamics, planetary waves, and upper-ocean mixing, in addition to important ocean-atmosphere feedbacks (Vecchi et al., 2004).

The hypothesized central role that oceanographic processes in the northern Arabian Sea play in the seasonal modulation of the Asian monsoon is accompanied by the realization that new in situ observations of currents, air-sea interactions, and meso- to submesoscale interior processes are needed to improve our physical understanding and our ability to forecast oceanic and atmospheric conditions in the region.

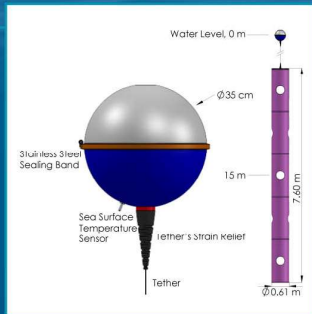
In situ oceanographic observations in the northern Arabian Sea have been difficult to obtain for over two decades because of piracy, with the notable exception of measurements from Global Climate Observing System subarrays such as the Global Drifter Program (GDP), Argo, the High-Resolution Expendable Bathythermograph/Expendable Conductivity-Temperature-Depth (HR XBT/XCTD) network, the Research Moored Array for African-Asian-Australian Monsoon Analysis and Prediction (RAMA; McPhaden et al., 2009), and the developing Indian Ocean Observing System (IndOOS) effort in the northeastern

Arabian Sea. Although the frequency of piracy incidents is declining, the region from the east coast of Africa to the central Arabian Sea (65°E) and from 5°S to 22°N is classified as high risk by the United Kingdom Hydrographic Office, and access by scientific research vessels remains restricted, particularly in the oceanographically critical regions of the Somali Current, the Red Sea, the Persian Gulf outflows, and the Arabian Peninsula upwelling system.

The complexity of the physical processes involved and the need to collect observations on scales ranging from one meter to thousands of kilometers in a region that is difficult to access with oceanographic research ships require a novel approach. The central objectives of the NASCar initiative are to exploit state-of-the-art autonomous instruments (Box 1) to address outstanding scientific questions about oceanographic processes in the northern Arabian Sea, to fill the observational gap accrued over the past two decades, and to demonstrate the maturity of an approach that does not rely on the use of dedicated research vessels and fixed mooring installations.

Several key features differentiate the northern Indian Ocean from the Atlantic and Pacific Oceans and affect the air-sea fluxes of heat and momentum over the basin. The presence of land to the north limits the ocean's poleward transport of heat and upper-ocean ventilation (Schott et al., 2009). Furthermore, the weak zonal component of the equatorial trade winds leads to mean downwelling along the equator (Wang and McPhaden, 2017), which results in high SSTs throughout the tropical Indian Ocean. Another remarkable feature is the drastic difference in sea surface salinity (SSS) across the northern Indian Ocean sub-basins—the Arabian Sea and the Bay of Bengal (Figure 1). In the northern Arabian Sea, evaporation largely exceeds precipitation, while

Box 1. Autonomous NASCar Assets



Surface Lagrangian SVP Drifter

SVP drifters use drogues centered at 15 m depth and are designed to follow the water with an accuracy of 0.01 m s^{-1} for winds up to 10 m s^{-1} . All drifters carry an SST sensor, and many of them also measure atmospheric pressure. Using two-way Iridium satellite communications, the data are available through the Global Telecommunication System in near-real time. They can also be configured to measure surface wind, salinity, and subsurface temperature. Undrogued drifters can measure directional spectral properties of surface waves. See <http://ltdl-drifter.org> for more details.



Profiling Floats

Profiling floats (standard Argo floats and the smaller, air-deployable ALAMO floats) use a buoyancy engine to move up and down in the water column. The pump moves oil from an internal reservoir to an external reservoir, changing the volume of the float and hence its density. A CTD on the float measures pressure, temperature, and salinity during its ascent. Profiling floats can be configured for a variety of profiling depths and frequency of cycling missions, and can be reprogrammed via two-way Iridium communication. See Jayne et al. (2017, in this issue), Jayne and Bogue (2017, in this issue), and <http://www.argo.ucsd.edu> for more details.



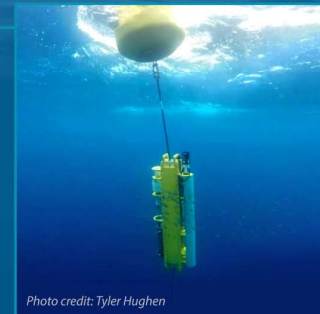
Underwater Gliders

Three varieties of autonomous underwater gliders (Rudnick, 2016) have been used during NASCar. Seagliders (Eriksen et al., 2001) measured temperature, salinity, and depth-averaged currents over the upper kilometer during missions lasting up to eight months. A Spray glider (Sherman et al., 2001; Rudnick et al., 2016) focused on sampling near the equator during a three-month mission. In addition to a CTD, the Spray glider carried a small acoustic Doppler current profiler (Todd et al., 2017) to measure profiles of horizontal currents near the equator where geostrophic estimates are not possible. A Slocum glider with an externally mounted turbulence package (Wolk et al., 2009; Fer et al., 2014) collected profiles of the dissipation rate of turbulent kinetic energy in the vicinity of the Mascarene Plateau during a month-long mission. All gliders telemetered real-time data via the Iridium network, and raw data are processed after recovery of the gliders.



HR-XBT

XBTs provide temperature profiles from the near surface to about 800 m depth, with drops from ships of opportunity spaced 20–30 km apart on the frequently repeated (~7–10 times per year) transect IX12 from Fremantle, Australia, to the Red Sea. Overall, around 250–350 XBT profiles are available along IX12 in any month of the year. The closely spaced “HR” hydrographic profiles are used to study the time variability of geostrophic transport (0–800 m) of the coastal boundary current system in the Arabian Sea.



Wirewalker Wave-Powered Profilers

The Wirewalker profiling system uses energy from surface ocean waves to drive a vehicle vertically along a wire. In the case described here, a pair of Wirewalkers was configured to profile temperature, conductivity, and pressure over 120 m and 200 m with a profile return rate of 12 min and 20 min, respectively, and telemeter the data over the Iridium satellite. See Pinkel et al. (2011) for more details.



Miniature Wave Buoys

The Miniature Wave Buoy (MWB) is a compact, inexpensive, easy-to-deploy/recover, oceanographic buoy that uses state-of-the-art GPS technology to measure waves. Significant wave heights up to 16 m and wave frequencies between 1 sec and 20 sec have been reported. MWBs support moored or drifting deployments of up to one year. Sampling rate, types of spectral data reported, and reporting intervals are user configurable. Spectra and sea state data are transmitted via the Iridium satellite network, and are available to users through the MWB website or by email.

the opposite is true in the Bay of Bengal, which is also affected by runoff from major rivers, resulting in SSS differences between the northern Arabian Sea and Bay of Bengal in excess of 5 psu (Gordon et al., 2016).

In the northern Arabian Sea, a strong southwesterly atmospheric jet, known as the Findlater jet (Findlater, 1969), develops during the summer southwest monsoon, with associated strong positive (negative) wind stress curl on its northwest (southeast) side, and induces strong upwelling off the coasts of Somalia and the Arabian Peninsula as well as downwelling to the southwest of the jet. The strong southwest monsoon winds and associated downwelling cause summertime

surface mixed layer deepening in about the same region where wintertime cooling and northeast monsoon winds create a deep mixed layer in winter (Figure 1c), resulting in a unique pattern of semi-annual mixed layer deepening in the northern Arabian Sea.

The northern Arabian Sea circulation and its western boundary current, the Somali Current, are strongly seasonal in response to the monsoon reversal (Schott et al., 2009). The southwest monsoon is associated with the powerful northward Somali Current, along with northward cross-equatorial flow that separates from the coast at about 3°N and 10°N to form the Southern Gyre and Great Whirl, respectively. During the northeast

monsoon, the reversed wind forcing is associated with a weaker southward Somali Current. During the two intermonsoon periods (i.e., approximately March–April and October–November), westerly equatorial winds result in equatorial ocean convergence and the eastward surface “Wyrтки jets” (Wyrтки, 1973).

Differences of the phasing of the northern Arabian Sea winds and the Somali Current boundary current system show that much remains to be understood about the physics of the seasonal current evolution, which includes remote forcing through planetary waves and cross-equatorial flow of the East African Coastal Current as well as seasonal asymmetry in the strength of the southwest versus the

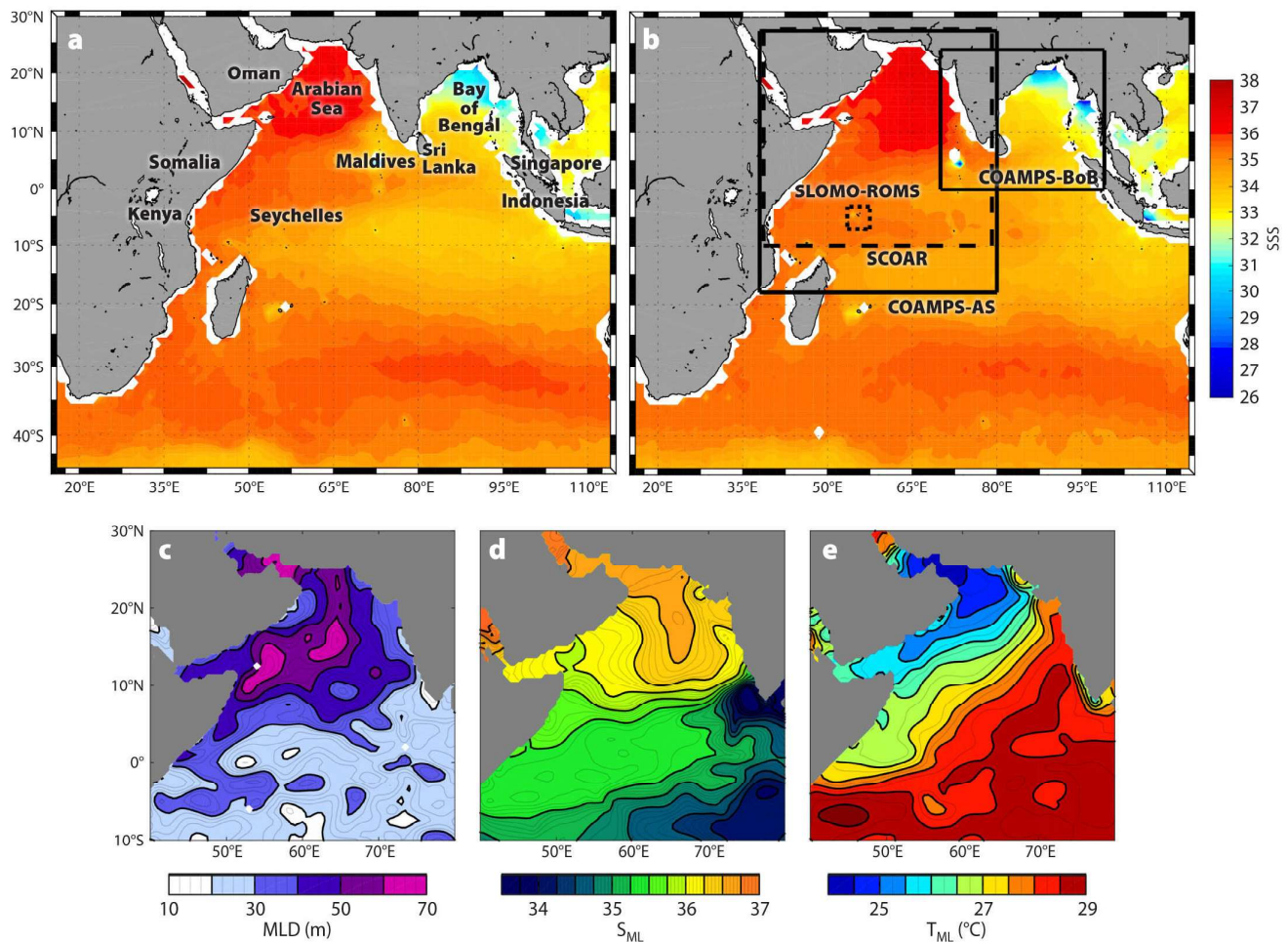


FIGURE 1. Mean remotely sensed sea surface salinity (SSS; 2012–2014) from the Aquarius satellite mission (T. Lee et al., 2012) during the (a) northeast monsoon (January–February), and (b) southwest monsoon (July–August). Several model domains (see Box 2) are superimposed in (b). Climatological mixed layer properties in January from the Argo-based Monthly Isopycnal/Mixed-layer Ocean Climatology (MIMOC; Schmidtke et al., 2013). (c) Depth. (d) Salinity. (e) Temperature.

northeast monsoon forcing. Reversal of the Somali Current from its southward northeast monsoon state can occur as early as March, before the onset of the summer monsoon. The early reversal of the Somali Current cannot be explained by westward-propagating, equatorially trapped Rossby waves (Lighthill, 1969; Leetmaa, 1972). Instead, annual downwelling Rossby waves, initiated during the previous southwest monsoon and propagating westward from the tip of India in November, may be responsible for its early reversal (Beal et al., 2013). NASCar is focusing closely on the Somali Current system seasonal evolution through observations and modeling to further refine these descriptions and hypotheses.

The remarkable seasonal changes of the northern Arabian Sea surface circulation cause interbasin exchanges of water masses that lead to interleaving and frontal features. Saline waters from the northwestern Arabian Sea meet the wintertime influx of fresher Bay of Bengal water at a broad salinity front crossing the northern Arabian Sea (Figure 1). There, high SSS destabilizes the stratification, contributing to the semiannual deepest and coolest mixed layers compared with the thinner and warmer mixed layers in the eastern northern Arabian Sea, which are influenced by the fresher, highly stratified Bay of Bengal inflow. Waters of different salinities (but similar densities) interleave vertically and create strong thermohaline stratification of different types, including barrier layers (Lukas and Lindstrom, 1991) and double diffusive layering (e.g., Schmitt, 1994).

In a barrier layer, strong salinity stratification creates a surface mixed layer within a deeper isothermal layer. Persistent barrier layers of about 40 m thickness in the southeastern part of the northern Arabian Sea that are associated with the fresh Bay of Bengal inflow (Figure 1e; de Boyer Montégut et al., 2014) can reduce vertical heat fluxes through the base of the mixed layer, allowing for higher SSTs. A mini warm pool, characterized by high SSTs (>30°C), develops through this

mechanism in the southeastern Arabian Sea and is linked to the monsoon onset vortex (Rao and Sivakumar, 1999). In contrast, barrier layers in the central northern Arabian Sea during the southwest monsoon are associated with much deeper mixed layers and weaker overall stratification. These barrier layers are less persistent and likely play a lesser role in atmospheric feedbacks. On the other hand, the “tilting” mechanism (Cronin and McPhaden, 2002), likely responsible for formation of barrier layers in the central Arabian Sea, may also be relevant for water mass subduction and ventilation of intermediate water masses in the basin.

Other thermohaline arrangements, often marked by temperature and salinity inversions, can create conditions for enhanced vertical mixing through double diffusion, a form of convective mixing arising from the differences in molecular diffusivities of heat and salt. Depending on whether the salinity or the temperature stratification is inverted, double diffusion takes the salt-fingering or the thermal-diffusive form. Introduction of high-salinity water through evaporation and nearby marginal sea outflows makes salt fingering more prevalent in the northern Arabian Sea and could facilitate lower SSTs, in contrast to barrier layers that facilitate higher SSTs.

The thermohaline structures of the northern Arabian Sea, the strong upwelling off the coasts of Somalia and Oman (C.M. Lee et al., 2000; Schott et al., 2009), and the swift (in excess of 2 m s⁻¹) northward Somali Current all contribute to modulation of the air-sea fluxes over large parts of the Arabian Sea. This modulation, in turn, affects the atmospheric moisture transport and subsequent changes in precipitation over South Asia and particularly the Indian subcontinent (Izumo et al., 2008), one of the most densely populated regions of the world. Improving the accuracy of marine and atmospheric predictions is therefore important for society as well as for commercial navigation and associated security-at-sea operations in an area of piracy activities.

SCIENTIFIC HYPOTHESIS AND PROGRAM DESIGN

NASCar was designed around three main hypotheses:

Hypothesis 1. The SST anomalies observed along the coast of Somalia, in the Great Whirl region, and off the coast of Oman affect ocean-atmosphere moisture fluxes (Vecchi et al., 2004), which can trigger intraseasonal oscillations of the southwest monsoon.

An accurate determination of the occurrence and strength of these SST anomalies requires advanced understanding of the dynamics of the Somali Current and its variability, connectivity to the interior northern Arabian Sea circulation, and energetics.

Hypothesis 2. Increasing mixed layer temperatures in the northern Arabian Sea trigger the onset of the southwest monsoon in spring.

The rate of warming, and therefore the timing and character of the monsoon, depends on the upper-ocean vertical structure. SSS gradients affect the temperature structure of the upper northern Arabian Sea through horizontal thermohaline filamentation and vertical interleaving driven by mesoscale and sub-mesoscale dynamics. Fresh barrier layers can enhance springtime warming, while mixing them away allows the ocean to cool. In contrast, high salinities in the northwestern Arabian Sea lead to salinity destabilization and widespread double diffusion, enhancing surface cooling or slowing warming.

Hypothesis 3. Kelvin waves generated in the western equatorial region during the intermonsoon periods, and Rossby waves generated at the eastern boundary (Sumatra) and Indian coast, connect the western and eastern basins in the northern Indian Ocean.

Upper-layer current and wind reversals drive interbasin exchanges south of Sri Lanka. The combination of mesoscale activity related to planetary waves

and interbasin exchanges sets water mass properties of the mini warm pool west of India, where strong modulation of the subsequent year's monsoon can occur.

Based on these scientific hypotheses, the northern Indian Ocean has been partitioned into four regions (Figure 2), each targeted with dedicated autonomous assets described in Box 1. The meteorological and modeling (Box 2) components are discussed separately.

Region 1. The Somali Boundary Current System

To address Hypothesis 1, this NASCar component is concerned with collecting observations of the oceanic inter- and intraseasonal variability of the Somali Current region for at least three seasonal cycles. The ultimate goal is to assess the relative importance of local

and remote forcing, to establish how and when the Somali Current connects with the interior Arabian Sea, and to validate the numerical models, which, in turn, are utilized to describe in full the seasonal development of the Somali boundary current system. The main observational tools are Surface Velocity Program (SVP) Lagrangian drifters, Argo and Air-Launched Autonomous Micro-Observer (ALAMO) profiling floats, XBTs, and expendable Wave Buoys. In recent years, the deployment rate of GDP drifters in the Arabian Sea has declined in connection with incidents of piracy. NASCar is relying on regular monthly to biweekly deployments of SVP drifters and on other autonomous assets deployed from Voluntary Observing Ships departing from Mombasa, Kenya. Other deployment opportunities are provided by the US Navy and the US Naval

Oceanographic Office. Wind stress measurements from satellite synthetic aperture radar (SAR) images complement the in situ ocean observations.

Region 2. Interior Dynamics of the Northern Arabian Sea

To address Hypothesis 2 and assess the skill of current-generation numerical models, a focused and coordinated multiplatform Lagrangian drift experiment using drifters, gliders, and floats was conducted to study the structure and dynamics of the upper ocean in the central part of the northern Arabian Sea down to about 200 m depth. A target area (12°N–15°N, 60°E–65°E) with a high concentration of interleaving features and deep mixed layers was identified based on historical data and models. The experiment is described in detail in Box 3.

Region 3. The Equatorial Region and the Mascarene Plateau

This component has been designed to address questions of how large-scale ocean processes interact with the atmospheric surface layer through instabilities, turbulence, and vertical advection/subsidence over different time scales, and how these phenomena couple with upper-ocean mixing processes to drive surface heat, moisture, and momentum fluxes (i.e., addressing Hypotheses 1 and 3). New Global Climate Observing System observations (i.e., Argo and GDP arrays; RAMA moorings at 66°E) are complemented by (1) autonomous underwater gliders with repeated occupations of sections between the Seychelles, Oman, and the Maldives to sample latitudinal and longitudinal contrasts in upper-ocean structures associated with the monsoon forcing, and (2) a pair of rapidly profiling, drifting Wirewalker systems (Pinkel et al., 2011; Lucas et al., 2016) deployed at 1°S, 55.5°E to investigate diurnal cycling in the mixed layer and fine-scale temperature and salinity interleaving in the thermocline along the equator.

Embedded in the equatorial circulation

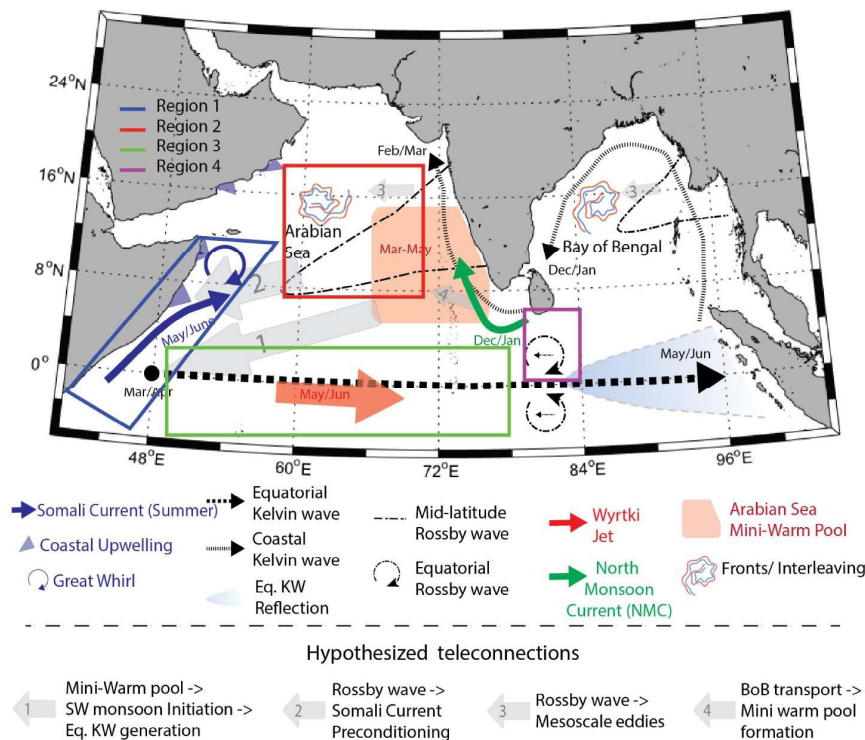


FIGURE 2. Schematic of the processes and hypothesized teleconnections between the Arabian Sea, the Bay of Bengal, and the equatorial Indian Ocean. Physical processes consist of a combination of planetary waves, seasonal-to-subseasonal atmospheric variability, and air-sea interactions that are preconditioned by each region's unique mixed layer, as well as thermohaline and thermocline characteristics. The Northern Arabian Sea Circulation-autonomous research (NASCar) initiative regions referenced in the text are also shown.

and planetary wave regime, the complex and seasonal circulation of the Seychelles, which lie atop the broad, shallow Mascarene Plateau (Figure 3c), represent a significant modeling challenge. The Seychelles Local Ocean Modeling and Observations (SLOMO) component focuses on the development of predictive capabilities of the region. SLOMO, in partnership with the Seychelles, is developing a foundational data set for regional- and local-scale modeling efforts, while providing guidance for the larger-scale

NASCAR efforts. Relevant processes include variability in surface waves, currents, stratification, and the seasonal internal wave climate, as well as connection of these processes with the large-scale oceanic circulation. The SLOMO array (i.e., moored acoustic Doppler current profilers, thermistors, CTDs, acoustic Doppler velocimeters, and occasional releases of autonomous CODE-style drifters [Davis, 1985]) were deployed in December 2015 along with vessel-based hydrographic surveys.

Region 4. Northern Arabian Sea/ Bay of Bengal Interbasin Exchanges and Connectivity

Two primary pathways for the export of surface Bay of Bengal freshwater are thought to exist. The indirect path follows the eastern boundary of the Bay of Bengal, spreading southward along the western rim of the Indonesian maritime continent and then turning westward within the tropical latitudes to reach the western margins of the Indian Ocean. The direct, seasonal path follows the

Box 2. NASCAR Numerical Modeling

The complex local and remote processes that influence the Arabian Sea circulation challenge a single numerical ocean general circulation model (OGCM) to realistically simulate flows over the broad range of spatial and temporal scales that characterize this basin. The NASCAR modeling efforts aim to enhance understanding of physical processes in the Arabian Sea so that reliable ocean forecasts can be developed. A range of ocean model simulations are being used that are strongly eddy-active, forced either by atmospheric reanalysis or fully coupled to an active atmospheric model on both regional and global grids, with some using data assimilation. Figure 1b shows the model domains. A summary of key modeling approaches follows.

Regional Coupled Models

Two regional configurations of the US Navy's Coupled Ocean-Atmosphere Mesoscale Prediction System (COAMPS) have been used to provide daily nowcasts since June 2015. COAMPS includes fully coupled atmosphere, ocean, and surface wave submodels that exchange fluxes every 10 minutes as well as tides and assimilated atmospheric and oceanic observations using 3Dvar with a 12-hour update cycle (Jensen et al., 2016). The goal is to study the impact of westward-propagating equatorial waves on eddies, the Somali boundary current system, resulting air-sea interactions and water exchanges between the Arabian Sea and the Bay of Bengal.

The Scripps Coupled Ocean-Atmosphere Regional (SCOAR WRF-ROMS) model (Seo et al., 2014) has been run for the 2001–2010 period (and is being extended to the NASCAR period) to examine scale-dependence of air-sea coupling in the Arabian Sea (Seo, in press). Scale separation of the coupling is enabled via an online, two-dimensional LOWESS filter (Seo et al., 2016) that is applied to SST and currents at every coupling interval (six-hour), allowing for a robust assessment of small-scale coupling effects on the circulation of the Arabian Sea. It features a 9 km resolution for both the ocean and the atmosphere, with matching grids and land-sea mask.

Global Ocean Model

A global 0.1° Parallel Ocean Program (POP) simulation, coupled to a sea ice model (CICE), run in the Community Earth System Modeling (CESM) framework, and forced with atmospheric reanalysis for 60 years, is used to understand how the dominant dynamics of the Somali Current system vary spatially along the African coast and with season by constructing full monthly momentum budgets from the archived POP runs. This model is also being used to understand changes in the circulation and

the potential vorticity in the central Arabian Sea. Output from a high-resolution preindustrial climate model simulation using these same 0.1° POP/CICE components in the Accelerated Climate Model for Energy (ACME) v0.1 is used to examine changes in the Somali Current circulation arising from interannual variability associated with large-scale climate modes influencing the circulation of the Arabian Sea.

Regional Ocean Model

The Regional Ocean Modeling System (ROMS) has been set up for the Seychelles with a stretched grid ranging from 1 km around the main islands of the Seychelles to 5 km offshore, with 16 surface-intensified vertical levels, and validated with SLOMO observations. The goal is to investigate the local circulation and water mass properties.

Ensemble Regional Modeling and Optimal Planning System

The MIT Multidisciplinary Simulation, Estimation, and Assimilation System (MSEAS; Haley and Lermusiaux, 2010; Haley et al., 2015) was used in real time for February–April 2017, issuing three-day ensemble ocean forecasts daily. MSEAS provided multiresolution downscaling from HYCOM (1/12°) to high-resolution nested and tiled domains, including tidal forcing, implicit two-way nesting, and 50 to 200 member ensembles, from 1/25° to 1/225° resolution. The ocean fields and their uncertainties were input to the MIT Optimal Planning System (NASCAR-OPS) to provide forecasts of reachable sets, reachability fronts, and probabilistic paths of gliders and floats (Lermusiaux et al., 2016, 2017, in this issue). MSEAS and NASCAR-OPS are used for optimal path planning and to guide persistent ocean sampling with autonomous vehicles as well as to quantify the dynamics and variability of circulation features.

Large Eddy Simulations (LES)

Vertical turbulent mixing processes that govern SST on hourly to weekly time scales are investigated with LES and turbulence closure modeling, coupled through model-data comparison. LES has column model geometry and horizontal domains of several hundred meters to resolve mixed layer turbulence in diurnal cycling down to orders of 1 m in long-time simulations. Of particular interest are forcing input from surface waves and the balance between surface evaporation and the horizontal divergence of salinity fluxes carried by laterally mixing submesoscale ocean processes.

western boundary of the Bay of Bengal around the southern tip of Sri Lanka and directly into the Arabian Sea. This NASCar component, focused on inter-basin exchange, relates to Hypotheses 2 and 3 and seeks to understand the relative importance of the two pathways. The Bay of Bengal freshwater reaching into the western tropical Indian Ocean eventually spreads into the western Arabian Sea, primarily in boreal summer. Salt input from the Arabian Sea to the Bay of Bengal passes along the southern tip

of Sri Lanka within the thermocline, mostly in the 50–150 m depth range (e.g., Wijesekera et al., 2015). Recent observations point to the existence of a seasonally reversing undercurrent east of Sri Lanka (Arachaporn Anutaliya, Scripps Institution of Oceanography, *pers. comm.*, 2017) that could provide a means of salt exchange between the Bay of Bengal and the Arabian Sea.

NASCar augments the existing Global Climate Observing System network with autonomous sampling by drifters, gliders,

floats, Pressure Inverted Echo Sounders (PIES), and drifting profilers. Multiyear occupation of a transect along 80.5°E between the southern tip of Sri Lanka and 2°N has been maintained by Seagliders at 20-day intervals and a pair of PIES near the ends of the transect.

To address the inherent challenges of comparing in situ observations and model output, NASCar also includes a Lagrangian particle tracking approach (Döös et al., 2013), where virtual particles are seeded offline in simulated

Box 3. NASCar Coordinated Multi-Platform Lagrangian Drift

Vertical interleaving, frontal subduction, and barrier layer formation are difficult to observe within a strong mesoscale eddy field (Shcherbina et al., 2015). Adopting a Lagrangian frame of reference in the near surface nullifies mesoscale advection and permits detailed investigations of the structure and evolution of small-scale features (Shcherbina et al., 2009).

An array consisting of 10 SVP barometer (SVPB) drifters, two Seagliders, five ALAMO floats, and 12 APEX floats was deployed in the northern Arabian Sea along a 1,300 km line crossing the target area from northwest to southeast (Figure 1c) from a ship of opportunity (US Naval Oceanographic Office) during the 2017 intermonsoon season.

Two ALAMO floats, rapidly profiling between 0 m and 300 m depth, provided a Lagrangian frame of reference (mixed layer and upper pycnocline) every two hours. Remarkably, the floats stayed within a few kilometers of each other throughout their 50-day, 325 km drift (Figure B3-1). See online supplemental material for an animation of their tracks.

Two Seagliders, profiling to 1,000 m every four to five hours, followed the target floats; they navigated a 20 km × 20 km “bowtie” pattern in the Lagrangian reference frame and provided a synoptic three-dimensional

context for the high-resolution float measurements. The navigation was handled by an automated system that ingested real-time asset locations, made a statistical forecast of the reference frame translation, transformed the survey pattern from the Lagrangian reference frame to geographic coordinates, and transmitted the navigation information to the gliders. The forecasts were fairly accurate (Figure B3-1), owing to rather simple and predictable mesoscale advection and weak wind forcing during this particular deployment.

To assist the ALAMO floats and Seaglider operations, the future float positions and the glider reachability sets were forecasted daily (see http://mseas.mit.edu/Sea_exercises/NASCar-OPS-17). To account for uncertainties, ensemble forecasts (Lermusiaux, 2007) were issued and the dynamic probability of float positions and of reachable points for the gliders were computed in real time (Lermusiaux et al., 2017, in this issue). The overall Lagrangian reachability planning system showed predictive skills for long periods of time. The skill was mostly governed and limited by the accuracy of the larger mesoscale field.

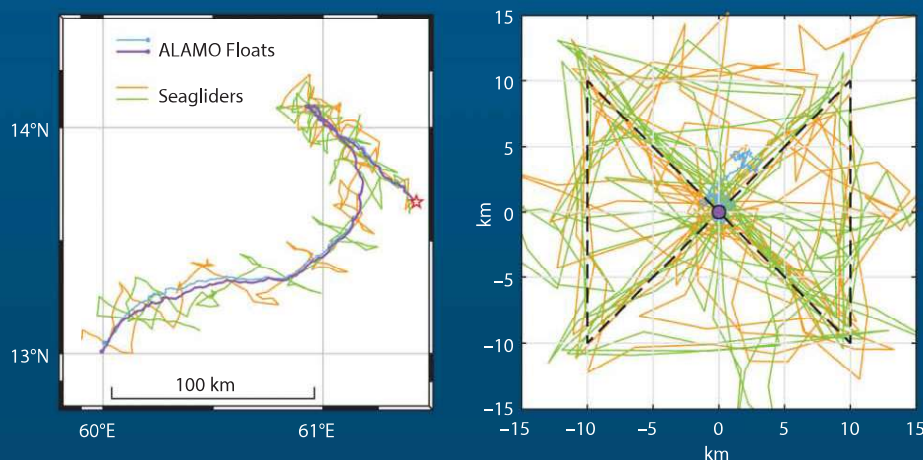


FIGURE B3-1. Trajectories of the ALAMO floats and the Seagliders during the coordinated Lagrangian drift (March 4–April 23, 2017) in geographic coordinates (left) and in the Lagrangian reference frame (right) following the ALAMO floats.

velocity fields generated by the global HYbrid Coordinate Ocean Model (HYCOM) with 1/12° spatial and daily temporal resolutions.

Meteorological Component

In addition to the SAR measurements in the Somali Current region, multiple daily radio soundings, a meteorological flux tower, and remote sensors (i.e., scanning Doppler LiDAR, microwave radiometer, and ceilometer) were deployed in the southern Arabian Sea (Seychelles), the western Bay of Bengal (Sri Lanka), and the eastern equatorial Indian Ocean (Singapore) between February 1 and March 15, 2015, with the goal of resolving intraseasonal (i.e., 10–45 day) and faster oscillations. These observations will aid in understanding the spatial extent and implications for SST of anomalous (downward) air-sea heat fluxes (Bhat and Fernando, 2016) in the northern Arabian Sea under high-wind conditions, and they will also provide valuable data for the validation of the numerical models used in NASCar (Box 2).

NASCar PRELIMINARY FINDINGS

NASCar’s autonomous data collection and modeling are currently underway (Figure 3). Some early results are described here.

Region 1. The Somali Boundary Current System

The northern Arabian Sea boundary current system, including the Somali Current, varies greatly with latitude. Sea level anomaly observations reveal that the mean width of the boundary current system decreases from about 300 km at 17°N at the coast of Oman to 60 km at the Somali coastline near 4°N. Ongoing drifter releases targeting the Somali boundary current system will define the spatial structure of the surface flow and the timing of the seasonal reversal of the surface flow.

The Somali Current between the equator and 10°N is dynamically divided into three regions: equatorial, central, and northern. Models (i.e., eddy-active ocean general circulation models) suggest that the reversal processes and timing vary

with regions. The flow in the northern part (6°N–10°N) is the first to reverse from equatorward to poleward during early boreal spring, due to the arrival of a downwelling Rossby wave propagating from the tip of India, and may reverse even earlier than this due to northward shear persisting from the previous season. South of about 2°N, the flow also reverses earlier than the local wind, whereas it closely matches the timing of the wind reversal in the central region between 2°N and 6°N. HR-XBT temperature profiles are revealing new fine-scale subsurface currents near the Somali coast. The precursor of the strong northward Somali Current observed in April has a significant subsurface southward countercurrent at depth. Model results also show a system of strong seasonal subsurface countercurrents, depending on their Somali Current region.

Regional coupled models indicate that currents and SSTs in the western part of the northern Arabian Sea are dynamically coupled to the atmosphere at distinct spatial scales (Seo et al., 2008; Seo,

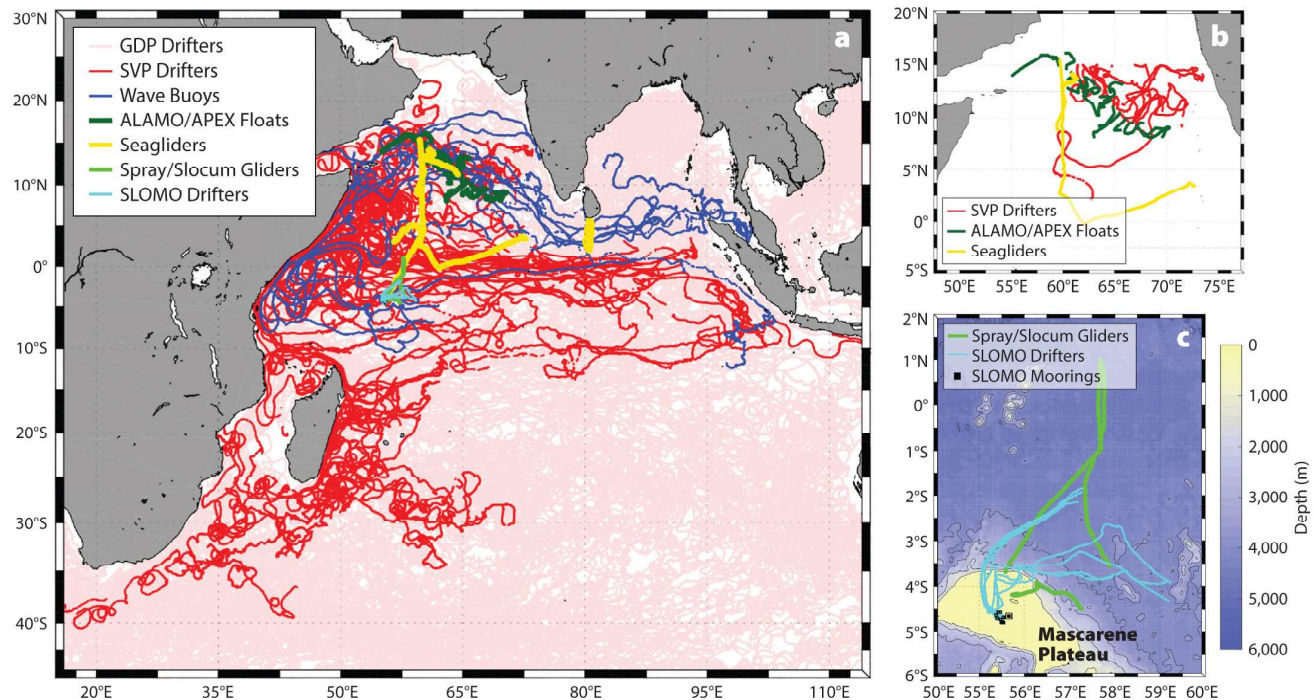


FIGURE 3. (a) Tracks and locations of NASCar autonomous assets. Details are shown of (b) the coordinated multi-platform Lagrangian drift (Region 2, and Box 3), and (c) Seychelles Local Ocean Modeling and Observations (SLOMO; Region 3).

in press). SST-wind coupling is strong on the oceanic mesoscale, affecting the position of the Great Whirl and the separation latitude of the Somali Current, while current-wind coupling attenuates the monsoon circulation and eddy activity. Furthermore, the moisture transport by the Findlater Jet is enhanced due to the current-wind coupling, suggesting that the current-induced air-sea interaction is important for simulation and prediction of monsoon rainfall over India. In situ surface current data from surface drifters will help to constrain the energetics of the surface flow to realistic estimates.

Further evidence of strong regional ocean-atmosphere coupling is provided by wind stress curl computed from the SAR data (Horstmann and Koch, 2005; Hersbach, 2010), showing strong positive curl associated with SST fronts. Bands of positive and negative wind stress curl, indicating organized large atmospheric eddies that arise from turbulent processes associated with a moderately unstable marine planetary boundary layer and aligned with the monsoon jet, occur over the southeastern part of the Somali Current region.

Region 2. Interior Dynamics of the Northern Arabian Sea (“Mixing Processes”)

The coordinated multi-platform Lagrangian drift experiment (Box 3) has revealed rich, vertical thermohaline interleaving structures in the upper 200 m. The numerous persistent thin layers support the strong tendency for salt fingering in the transition zone underlying the well-mixed surface layer. The observed fine-scale thermohaline structures suggest double-diffusive mixing, with uniform thermohaline gradients beneath warm, salty intrusions, and nearly isothermal haloclines above them (Figure 4). To support the Lagrangian experiment, multi-resolution ensemble ocean simulations (Lermusiaux, 2007; Haley et al., 2015) downscaled from HYCOM were run in real time. Forecasts showed that high-resolution (e.g., $1/75^\circ$ in the horizontal

with 70 or more optimized levels) were needed to develop and maintain such layered features.

On the larger scale, historical Argo data indicate salt-fingering-favorable conditions throughout the northwestern part of the northern Arabian Sea, both at the base of the saline surface layer and below, with the exception of the fresh Bay of Bengal inflow region. A quantitative index of active salt fingering, computed from historical Argo data and preliminary NASCar observations, shows that the layers are poised just below the critical value, with random, scattered forays into strong salt fingering, suggesting double diffusion is influencing vertical stratification.

Near the surface, preliminary results from Large Eddy Simulations (LES) of northern Arabian Sea diurnal cycling do not strongly support a significant role for wave breaking in setting near-surface vertical temperature gradients. Instead, it was found that including Langmuir turbulence in the LES accounts for most of the observed near-surface mixing attributable to waves. NASCar will elucidate the relative importance of turbulent mixing processes that set the regional SST properties.

Region 3. The Equatorial Region and the Mascarene Plateau

Observations from four glider surveys across the equator between 57.5°E and 62°E provide new insights into the seasonal evolution that occurs near the

equator (Figure 5). Water mass properties within 1° of the equator varied significantly during the eight-month period from August 2016 to May 2017, particularly shallower than the 26.0 kg m^{-3} isopycnal ($\sim 150 \text{ m}$, Figure 5a–i). A well-developed mixed layer with a thickness of about 50 m was present near the end of the southwest monsoon when the freshest near-surface waters were observed (Figure 5a,e,i). By January 2017, near-surface waters had become cooler and saltier, resulting in a surface density increase of nearly 1 kg m^{-3} and shoaling of the 24.0 kg m^{-3} isopycnal by about 50 m (Figure 5b,f,i).

During boreal spring, near-surface warming led to the warmest observed waters ($>30^\circ\text{C}$ by May 2017; Figure 5c,d,i). The saltiest waters observed within 1° of the equator were found at 50–100 m depth in April 2017 (Figure 5g,i). This salty layer thickened and spread southward in May 2017 (Figure 5h). The back-to-back transects across the equator between March and May 2017 highlight how quickly water mass properties can change as the southwest monsoon sets in. The density of the subsurface salinity maximum near 0.5°N decreased by 1 kg m^{-3} in 11 days (Figure 5i), while the high-salinity layer spread southward and upward between the two transects (Figure 5g,h). Absolute velocity profiles from the Spray glider (Todd et al., 2017) captured the shift in the equatorial circulation coincident with the abrupt shift

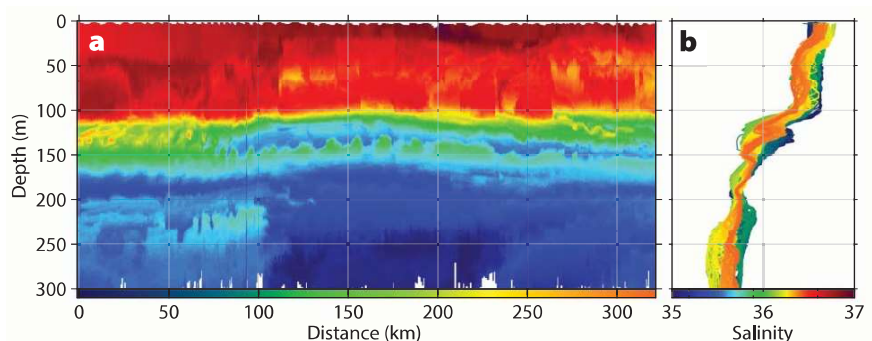


FIGURE 4. Salinity observations from an ALAMO float deployed during the coordinated multi-platform Lagrangian experiment reveal fine-scale interleaving of water masses. (a) Salinity profiles are shown along the track of the float, and (b) individual salinity profiles are color-coded by along-track distance.

in water mass properties during March–May 2017. The Equatorial Undercurrent, which carried high-salinity waters eastward, weakened from April to May. At the surface, currents south of the equator switched from westward to eastward, presumably as a Wyrtki jet developed.

The 2016 SLOMO observations highlight strong seasonal currents on the Mascarene Plateau, with variability dominated by near-inertial currents and not by tides, which are only a weak influence. The stratification varies semi-annually, as does the low-pass filtered

sea surface height. It is hypothesized that these semi-annual signals are tied to the monsoonal changes in the equatorial circulation. Local processes, such as high-frequency internal waves, are likely modulated by the monsoons with remote processes driving the stratification. CODE

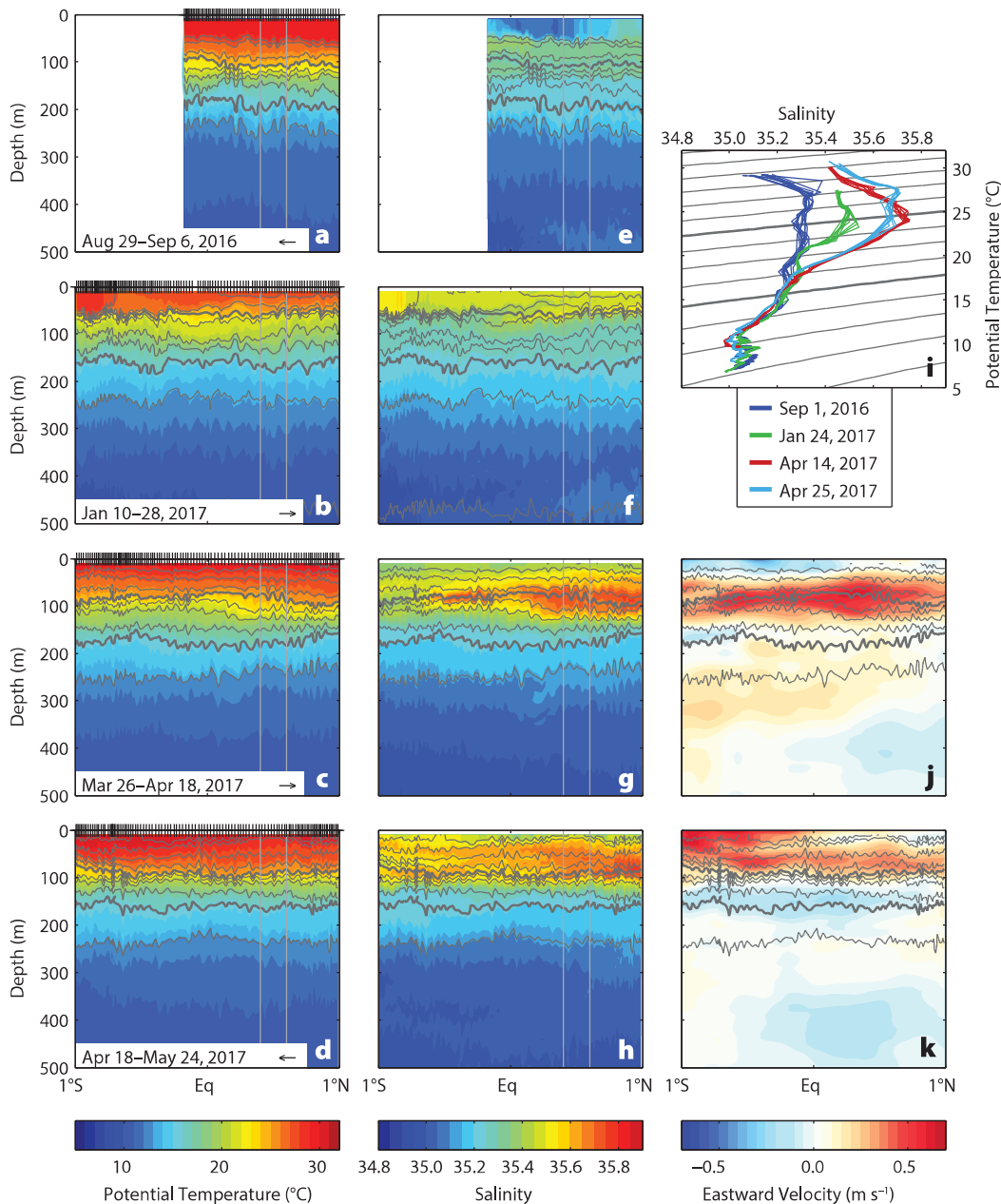


FIGURE 5. Equatorial observations collected by NASCar gliders. Transects of (a–d) potential temperature and (e–h) salinity in the upper 500 m are shown for four successive equator crossings, with dates and directions of glider transits denoted in a–d. (i) Potential temperature–salinity curves between 0.4°N and 0.6°N (vertical gray lines in a–h) from each glider transect with approximate dates indicated. (j–k) Eastward velocity measured by the Spray glider. In all panels, contours of potential density are drawn every 0.5 kg m⁻³ with the 24.0 kg m⁻³ and 26.0 kg m⁻³ isopycnals marked bold. Locations of individual profiles are denoted by tick marks at the top of panels a–d.

drifters released at the Seychelles further demonstrate connectivity between the plateau and the equatorial currents of the order of days (Figure 3c).

Region 4. Northern Arabian Sea/ Bay of Bengal Interbasin Exchanges and Connectivity

Exchanges and connectivity between the Arabian Sea and Bay of Bengal are being analyzed observationally using Argo floats, drifters, gliders, remote sensing of surface salinity and winds, moored arrays south of Sri Lanka, and in models using Lagrangian particle tracking. The observations show the spread of fresh Bay of Bengal waters along the two pathways into the Arabian Sea, as described in the program design section above.

Monthly releases of virtual surface drifters in near-surface velocity fields from HYCOM and advected for two years (2013–2015) suggest residence times for the Bay of Bengal and the northern Arabian Sea waters of about one month during boreal summer. Some of the exported waters return to the release regions in fall, and the sustained residence times based on the annual cycle are closer to a year. Waters originating in the Bay of Bengal reach the northern Arabian Sea between January and May in the year after seeding, whereas waters from the 2013 northern Arabian Sea release reached the Bay of Bengal from September 2013 to March 2014. In both cases, the drifter trajectories varied strongly with the timing of their release, thus confirming the importance of seasonal variability in the regional ocean circulation.

The connectivity between the Somali Current and the interior Arabian Sea, the tropical gyre south of the equator, and the Bay of Bengal is also studied with simulated surface drifter trajectories using the Lagrangian Tool Connectivity Modeling System (Paris et al., 2013) and monthly near-surface velocity fields from historical GDP data (Laurindo et al., 2017). A preliminary analysis of the simulations suggests little connectivity between the Somali Current

and the interior circulation (cf. Figure 3a) and confirms the occurrence of two distinct cross-equatorial gyres (see Schott and McCreary, 2001, or Schott et al., 2009, for schematics of the monsoon circulation). The first gyre results from surface waters branching eastward at about 3°N after crossing the equator in April and May and feeding into the South Equatorial Countercurrent, which is also reflected in the drifter trajectories shown in Figure 3a. Subsequently, these waters are driven southward by local winds and return to the western boundary via the South Equatorial Current after about one year. The second gyre results from surface waters crossing the equator from April to August and continuing north to feed into the Somali Current and the Great Whirl. From June to October, these waters flow southeastward and into the Bay of Bengal along the equator, recirculating via the North Monsoon Current. Eventually, the southwest monsoon drives these waters southward back across the equator. The return path to the western boundary is similar to that for the first gyre, with the whole circulation taking about two years.

SUMMARY

The NASCar initiative investigates complex oceanographic processes that contribute to the modulation of air-sea fluxes in the northern Arabian Sea and the associated impacts on the monsoon evolution and feedbacks. The observational program covers a wide range of spatial and temporal scales with in situ observations from autonomous instruments, and operates in an area where in situ observations have been sparse for the past two decades due to piracy concerns. NASCar is rapidly filling this notable data gap with a multi-pronged approach that merges autonomous ocean observations with ocean and coupled climate models, conceptual models, remote sensing, and meteorological observations. Optimal Planning Systems (Box 2) are used to assist the deployment and recovery of several autonomous assets and were also used for planning and guiding the coordinated Lagrangian

drift (Box 3; Lermusiaux et al., 2017, in this issue). Such an approach is becoming increasingly important as the use of autonomous platforms gains traction as a powerful and comprehensive alternative, as discussed here, to more traditional ship-based research programs. International collaborations and the use of Voluntary Observing Ships for deployments are key elements for maintaining multiyear time series at both basin and global scales. NASCar benefits from the decades of experience of programs such as the GDP that developed a global network of international partners based on the collaboration between oceanographers and meteorologists (Niiler, 2001; Centurioni et al., 2017) under the Data Buoy Cooperation Panel of the World Meteorological Organization as well as on the established tradition of international collaborations that are central to the success of several ONR programs.

Early results support the efficacy of the novel NASCar approach. For instance, the observations of thermohaline interleaving in the northern Arabian Sea are providing new insights into the importance of barrier layers and double diffusion in setting the vertical stratification and in influencing SST. Sustained glider and float measurements in the region will further elucidate the role of barrier layers and lateral mesoscale stirring/advection in creating SST anomalies.

Interbasin glider, wave buoy, and Wirewalker observations are complemented by larger-scale drifter and float data as well as remote-sensing products to establish a new baseline for elucidating the role of ocean-atmosphere processes in modulating and pre-conditioning the reversing monsoon circulation of the Arabian Sea and of the equatorial region, and for determining how mesoscale SST properties and energetics affect regional air-sea fluxes. Various numerical models will not only allow for a detailed and validated assessment of small-scale coupling in the circulation of the Arabian Sea and air-sea flux modulation but will also provide a detailed dynamical view

of the regional circulation that cannot be fully resolved by the NASCar observations alone. A joint analysis of models and observations will thus be central to enhancing forecasting skills for this complicated region.

SUPPLEMENTAL MATERIALS

YouTube video of coordinated drift during the NASCar experiment can be viewed at <https://youtu.be/WveJDHaS3g>.

REFERENCES

Beal, L.M., V. Hormann, R. Lumpkin, and G.R. Foltz. 2013. The response of the surface circulation of the Arabian Sea to monsoonal forcing. *Journal of Physical Oceanography* 43(9):2,008–2,022, <https://doi.org/10.1175/JPO-D-13-033.1>.

Bhat, G., and H.J. Fernando. 2016. Remotely driven anomalous sea-air heat flux over the North Indian Ocean during the summer monsoon season. *Oceanography* 29(2):232–241, <https://doi.org/10.5670/oceanog.2016.55>.

Centurioni, L., A. Horányi, C. Cardinali, E. Charpentier, and R. Lumpkin. 2017. A global ocean observing system for measuring sea level atmospheric pressure: Effects and impacts on numerical weather prediction. *Bulletin of the American Meteorological Society* 98(2):231–238, <https://doi.org/10.1175/bams-d-15-00080.1>.

Cronin, M.F., and M.J. McPhaden. 2002. Barrier layer formation during westerly wind bursts. *Journal of Geophysical Research* 107(C12), 8020, <https://doi.org/10.1029/2001JC001171>.

Davis, R.E. 1985. Drifter observations of coastal surface currents during CODE: The method and descriptive view. *Journal of Geophysical Research* 90(C3):4,741–4,755, <https://doi.org/10.1029/JC090iC03p04741>.

de Boyer Montégut, C., F. Durand, R. Bourdallé-Badie, and B. Blanke. 2014. Role of fronts in the formation of Arabian Sea barrier layers during summer monsoon. *Ocean Dynamics* 64(6):809–822, <https://doi.org/10.1007/s10236-014-0716-7>.

Döös, K., J. Kjellsson, and B. Jönsson. 2013. TRACMASS: A Lagrangian trajectory model. Pp. 225–249 in *Preventive Methods for Coastal Protection*. T. Soomere and E. Quak, eds, Springer, Heidelberg.

Eriksen, C.C., T.J. Osse, R.D. Light, T. Wen, T.W. Lehman, P.L. Sabin, J.W. Ballard, and A.M. Chiodi. 2001. Seaglider: A long-range autonomous underwater vehicle for oceanographic research. *IEEE Journal of Oceanic Engineering* 26(4):424–436, <https://doi.org/10.1109/48.972073>.

Fer, I., A.K. Peterson, and J.E. Ullgren. 2014. Microstructure measurements from an underwater glider in the turbulent Faroe Bank Channel overflow. *Journal of Atmospheric and Oceanic Technology* 31:1128–1150, <https://doi.org/10.1175/JTECH-D-13-00221.1>.

Findlater, J. 1969. A major low-level air current near the Indian Ocean during the northern summer. *Quarterly Journal of the Royal Meteorological Society* 95(404):362–380, <https://doi.org/10.1002/qj.49709540409>.

Gordon, A.L., E.L. Shroyer, A. Mahadevan, D. Sengupta, and M. Freilich. 2016. Bay of Bengal: 2013 northeast monsoon upper-ocean circulation. *Oceanography* 29(2):82–91, <https://doi.org/10.5670/oceanog.2016.41>.

Haley, P.J., A. Agarwal, and P.F.J. Lermusiaux. 2015. Optimizing velocities and transports for complex coastal regions and archipelagos. *Ocean Modelling* 89:1–28, <https://doi.org/10.1016/j.ocemod.2015.02.005>.

Haley, P.J., and P.F.J. Lermusiaux. 2010. Multiscale two-way embedding schemes for free-surface primitive equations in the “Multidisciplinary Simulation, Estimation and Assimilation System.” *Ocean Dynamics* 60(6):1,497–1,537, <https://doi.org/10.1007/s10236-010-0349-4>.

Hersbach, H. 2010. Comparison of C-band scatterometer CMOD5.N equivalent neutral winds with ECMWF. *Journal of Atmospheric and Oceanic Technology* 27(4):721–736, <https://doi.org/10.1175/2009JTECHO698.1>.

Horstmann, J., and W. Koch. 2005. Measurement of ocean surface winds using synthetic aperture radars. *IEEE Journal of Oceanic Engineering* 30(3):508–515, <https://doi.org/10.1109/JOE.2005.857514>.

Izumo, T., C. de Boyer Montégut, J.-J. Luo, S.K. Behera, S. Masson, and T. Yamagata. 2008. The role of the western Arabian Sea upwelling in Indian monsoon rainfall variability. *Journal of Climate* 21(21):5,603–5,623, <https://doi.org/10.1175/2008jcli2158.1>.

Jayne, S.R., and N.M. Bogue. 2017. Air-deployable profiling floats. *Oceanography* 30(2):29–31, <https://doi.org/10.5670/oceanog.2017.214>.

Jayne, S.R., D. Roemmich, N. Zilberman, S.C. Riser, K.S. Johnson, G.C. Johnson, and S.R. Piotrowicz. 2017. The Argo Program: Present and future. *Oceanography* 30(2):18–28, <https://doi.org/10.5670/oceanog.2017.213>.

Jensen, T.G., H.W. Wijesekera, E.S. Nyadjro, P.G. Thoppil, J.F. Shriver, K. Sandeep, and V. Pant. 2016. Modeling salinity exchanges between the equatorial Indian Ocean and the Bay of Bengal. *Oceanography* 29(2):92–101, <https://doi.org/10.5670/oceanog.2016.42>.

Laurindo, L.C., A.J. Mariano, and R. Lumpkin. 2017. An improved near-surface velocity climatology for the global ocean from drifter observations. *Deep Sea Research Part I* 124:73–92, <https://doi.org/10.1016/j.dsr.2017.04.009>.

Lee, C.M., B.H. Jones, K.H. Brink, and A.S. Fischer. 2000. The upper-ocean response to monsoonal forcing in the Arabian Sea: Seasonal and spatial variability. *Deep Sea Research Part II* 47(7–8):1,177–1,226, [https://doi.org/10.1016/S0967-0645\(99\)00141-1](https://doi.org/10.1016/S0967-0645(99)00141-1).

Lee, T., G. Lagerloef, M.M. Gierach, H.Y. Kao, S. Yueh, and K. Dohani. 2012. Aquarius reveals salinity structure of tropical instability waves. *Geophysical Research Letters* 39, L12610, <https://doi.org/10.1029/2012GL052232>.

Leetmaa, A. 1972. The response of the Somali Current to the southwest monsoon of 1970. *Deep Sea Research and Oceanographic Abstracts* 19:319–325, [https://doi.org/10.1016/0011-7471\(72\)90025-3](https://doi.org/10.1016/0011-7471(72)90025-3).

Lermusiaux, P.F.J. 2007. Adaptive modeling, adaptive data assimilation and adaptive sampling. *Physica D: Nonlinear Phenomena* 230(1):172–196, <https://doi.org/10.1016/j.physd.2007.02.014>.

Lermusiaux, P.F.J., P.J. Haley Jr., S. Jana, A. Gupta, C.S. Kulkarni, C. Mirabito, W.H. Ali, D.N. Subramani, A. Dutt, J. Lin, and others. 2017. Optimal planning and sampling predictions for autonomous and Lagrangian platforms and sensors in the northern Arabian Sea. *Oceanography* 30(2):172–185, <https://doi.org/10.5670/oceanog.2017.242>.

Lermusiaux, P.F.J., T. Lolla, P.J. Haley Jr., K. Yigit, M.P. Ueckeremann, T. Sondergaard, and W.G. Leslie. 2016. Science of autonomy: Time-optimal path planning and adaptive sampling for swarms of

ocean vehicles. Pp. 481–498 in *Springer Handbook of Ocean Engineering*. M.R. Dhanak and N.I. Xiros, eds, Springer International Publishing.

Lighthill, M.J. 1969. Dynamic response of the Indian Ocean to onset of the southwest monsoon. *Philosophical Transactions of the Royal Society of London A* 265(1159):45–92, <https://doi.org/10.1098/rsta.1969.0040>.

Lucas, A.J., J.D. Nash, R. Pinkel, J.A. MacKinnon, A. Tandon, A. Mahadevan, M.M. Omand, M. Freilich, D. Sengupta, and M. Ravichandran. 2016. Adrift upon a salinity-stratified sea: A view of upper-ocean processes in the Bay of Bengal during the southwest monsoon. *Oceanography* 29(2):134–145, <https://doi.org/10.5670/oceanog.2016.46>.

Lukas, R., and E. Lindstrom. 1991. The mixed layer of the western equatorial Pacific Ocean. *Journal of Geophysical Research* 96(S01):3,343–3,357, <https://doi.org/10.1029/90JC01951>.

McPhaden, M.J., G. Meyers, K. Ando, Y. Masumoto, V.S.N. Murty, M. Ravichandran, F. Syamsudin, J. Vialard, L. Yu, and W. Yu. 2009. RAMA: The Research Moored Array for African-Asian-Australian Monsoon Analysis and Prediction. *Bulletin of the American Meteorological Society* 90(4):459–480, <https://doi.org/10.1175/2008BAMS2608.1>.

Niiler, P.P. 2001. The world ocean surface circulation. Pp. 193–204 in *Ocean Circulation and Climate*. G. Siedler, J. Church and J. Gould, eds, Academic Press.

Paris, C.B., J. Helgers, E. Van Sebille, and A. Srinivasan. 2013. Connectivity Modeling System: A probabilistic modeling tool for the multi-scale tracking of biotic and abiotic variability in the ocean. *Environmental Modelling & Software* 42:47–54, <https://doi.org/10.1016/j.envsoft.2012.12.006>.

Pinkel, R., M.A. Goldin, J.A. Smith, O.M. Sun, A.A. Aja, M.N. Bui, and T. Hughen. 2011. The Wirewalker: A vertically profiling instrument carrier powered by ocean waves. *Journal of Atmospheric and Oceanic Technology* 28:426–435, <https://doi.org/10.1175/2010JTECHO805.1>.

Rao, R.R., and R. Sivakumar. 1999. On the possible mechanisms of the evolution of a mini-warm pool during the pre-summer monsoon season and the genesis of onset vortex in the South-Eastern Arabian Sea. *Quarterly Journal of the Royal Meteorological Society* 125(555):787–809, <https://doi.org/10.1002/qj.49712555503>.

Rudnick, D.L. 2016. Ocean research enabled by underwater gliders. *Annual Reviews of Marine Science* 8:519–541, <https://doi.org/10.1146/annurev-marine-122414-033913>.

Rudnick, D.L., R.E. Davis, and J.T. Sherman. 2016. Spray underwater glider operations. *Journal of Atmospheric and Oceanic Technology* 33:1,113–1,122, <https://doi.org/10.1175/jtech-d-15-0252.1>.

Schmidtko, S., G.C. Johnson, and J.M. Lyman. 2013. MIMOC: A global monthly isopycnal upper-ocean climatology with mixed layers. *Journal of Geophysical Research* 118(4):1,658–1,672, <https://doi.org/10.1002/jgrc.20122>.

Schmitt, R.W. 1994. Double diffusion in oceanography. *Annual Review of Fluid Mechanics* 26(1):255–285, <https://doi.org/10.1146/annurev.fl.26.010194.001351>.

Schott, F.A., and J.P. McCreary. 2001. The monsoon circulation of the Indian Ocean. *Progress in Oceanography* 51(1):1–123, [https://doi.org/10.1016/s0079-6611\(01\)00083-0](https://doi.org/10.1016/s0079-6611(01)00083-0).

Schott, F.A., S.-P. Xie, and J.P. McCreary Jr. 2009. Indian Ocean circulation and climate variability. *Reviews of Geophysics* 47(1), RG1002, <https://doi.org/10.1029/2007rg000245>.

Seo, H. In press. Distinct influence of air-sea interactions mediated by mesoscale sea surface temperature and surface current in the Arabian Sea. *Journal of Climate*, <https://doi.org/10.1175/jcli-d-16-0834.1>.

Seo, H., A.J. Miller, and J.R. Norris. 2016. Eddy-wind interaction in the California Current System: Dynamics and impacts. *Journal of Physical Oceanography* 46(2):439–459, <https://doi.org/10.1175/JPO-D-15-0086.1>.

Seo, H., R. Murtugudde, M. Jochum, and A.J. Miller. 2008. Modeling of mesoscale coupled ocean-atmosphere interaction and its feedback to ocean in the western Arabian Sea. *Ocean Modelling* 25:120–131, <https://doi.org/10.1016/j.ocemod.2008.07.003>.

Seo, H., A.C. Subramanian, A.J. Miller, and N.R. Cavanaugh. 2014. Coupled impacts of the diurnal cycle of sea surface temperature on the Madden-Julian oscillation. *Journal of Climate* 27(22):8,422–8,443, <https://doi.org/10.1175/JCLI-D-14-00141.1>.

Shcherbina, A.Y., M.C. Gregg, M.H. Alford, and R.R. Harcourt. 2009. Characterizing thermohaline intrusions in the North Pacific Subtropical Frontal Zone. *Journal of Physical Oceanography* 39(11):2,735–2,756, <https://doi.org/10.1175/2009jpo4190.1>.

Shcherbina, A.Y., M.A. Sundemeyer, E. Kunze, E. D'Asaro, G. Badin, D. Birch, A.-M.E.G. Brunner-Suzuki, J. Callies, B.T. Kuebel Cervantes, M. Claret, and others. 2015. The LatMix summer campaign: Submesoscale stirring in the upper ocean. *Bulletin of the American Meteorological Society* 96(8):1,257–1,279, <https://doi.org/10.1175/bams-d-14-00015.1>.

Sherman, J.T., R.E. Davis, W.B. Owens, and J. Valdes. 2001. The autonomous underwater glider "Spray." *IEEE Journal of Oceanic Engineering* 26(4):437–446, <http://doi.org/10.1109/48.972076>.

Todd, R.E., D.L. Rudnick, J.T. Sherman, W.B. Owens, and L. George. 2017. Absolute velocity measurements from autonomous underwater gliders equipped with Doppler current profilers. *Journal of Atmospheric and Oceanic Technology* 34(2):309–333, <https://doi.org/10.1175/JTECH-D-16-0156.1>.

Trott, C.B., B. Subrahmanyam, and V.S.N. Murty. 2017. Variability of the Somali Current and eddies during the southwest monsoon regimes. *Dynamics of Atmospheres and Oceans* 79:43–55, <https://doi.org/10.1016/j.jdynatmoce.2017.07.002>.

Vecchi, G.A., S.-P. Xie, and A.S. Fischer. 2004. Ocean-atmosphere covariability in the western Arabian Sea. *Journal of Climate* 17(6):1,213–1,224, [https://doi.org/10.1175/1520-0442\(2004\)017<1213:ocitwa>2.0.co;2](https://doi.org/10.1175/1520-0442(2004)017<1213:ocitwa>2.0.co;2).

Wang, Y., and M.J. McPhaden. 2017. Seasonal cycle of cross-equatorial flow in the central Indian Ocean. *Journal of Geophysical Research* 122, <https://doi.org/10.1002/2016JC012537>.

Wijesekera, H.W., T.G. Jensen, E. Jarosz, W.J. Teague, E.J. Metzger, D.W. Wang, S.U.P. Jinadasa, K. Arulananthan, L.R. Centurioni, and H.J.S. Fernando. 2015. Southern Bay of Bengal currents and salinity intrusions during the northeast monsoon. *Journal of Geophysical Research* 120(10):6,897–6,913, <https://doi.org/10.1002/2015JC010744>.

Wolk, F., R. Lueck, and L.C. St. Laurent. 2009. Turbulence measurements from a glider. In *OCEANS 2009, MTS/IEEE Biloxi - Marine Technology for Our Future: Global & Local Challenges*. October 26–29, 2009, Biloxi, Mississippi.

Wyrtki, K. 1973. An equatorial jet in the Indian Ocean. *Science* 181(4096):262–264, <https://doi.org/10.1126/science.181.4096.262>.

ACKNOWLEDGMENTS

We are grateful to Theresa Paluszkiwicz of the Office of Naval Research for her essential contributions and support. The authors were funded through NASCar DRI grants. Additional support from the Global Drifter Program, grant NA15OAR4320071 (L.C. VH); the CSL Laboratory at the NCAR CISEL (Yellowstone ark:/85065/d7wd3xhc) (JMC); and the Department of Energy ACME project DE-SC0012778 (JMC) are gratefully acknowledged. The US Navy, the US Hydrographic Office, CMA CGM SA, and the American President Line are acknowledged for deploying NASCar assets. Operational support in Kenya was provided by Joseph Odhiambo Amollo of the Kenya Meteorological Services, and in the Seychelles by the Better Life Foundation and the Seychelles Coast Guard, Priyantha Jinadasa (NARA, Sri Lanka), Bragg Sherrer, Joe Cotton (NAVO), the Maldives Coast Guard, the Whale Shark Research Institute and Meteorological Service, Bob Ashton (PROTEQ), Jason Gobat, Geoff Shilling, Ben Jokinen, Adam Huxtable, and Myles LeMaistre (all APL-UW) are gratefully acknowledged.

AUTHORS

Luca Centurioni (lcenturioni@ucsd.edu) is Associate Researcher, **Verena Hormann** is Project Scientist, **Lynne D. Talley** is Distinguished Professor, and **Isabella Arzeno** is a graduate student, all at Scripps Institution of Oceanography (SIO), University of California, San Diego, La Jolla, CA, USA. **Lisa Beal** is Professor and Associate Dean of Research, Rosenstiel School of Marine and Atmospheric Science (RSMAS), University of Miami, Miami, FL, USA. **Michael Caruso** is Senior Systems Engineer, Center for Southeastern Tropical Advanced Remote Sensing (CSTARS), University of Miami, Miami, FL, USA. **Patrick Conry** is a graduate student in the College of Engineering, University of Notre Dame, Notre Dame, IN, USA. **Rosalind Echols** is a graduate student in the School of Oceanography, University of Washington, Seattle, WA, USA. **Harindra J.S. Fernando** is Wayne and Diana Murdy Endowed Professor, College of Engineering, University of Notre Dame, Notre Dame, IN, USA. **Sarah N. Giddings** is Assistant Professor, SIO, University of California, San Diego, La Jolla, CA, USA. **Arnold Gordon** is Professor, Lamont-Doherty Earth Observatory of Columbia University, Palisades, NY, USA. **Hans Graber** is Professor and CSTARS Director, University of Miami, Miami, FL, USA. **Ramsey R. Harcourt** is Principal Oceanographer, Applied Physics Laboratory (APL), University of Washington, Seattle, WA, USA. **Steven R. Jayne** is Senior Scientist, Woods Hole Oceanographic Institution (WHOI), Woods Hole, MA, USA. **Tommy G. Jensen** is **Oceanographer, Naval Research Laboratory, Stennis Space Center, MS, USA.**

Craig M. Lee

is Senior Principal Oceanographer and Professor, APL, University of Washington, Seattle, WA, USA. **Pierre F.J. Lermusiaux** is Professor, Department of Mechanical Engineering, Massachusetts Institute of Technology, Cambridge, MA, USA. **Pierre L'Hegaret** is Postdoctoral Associate, RSMAS, University of Miami, Miami, FL, USA. **Andrew J. Lucas** is Assistant Professor, SIO, University of California, San Diego, La Jolla, CA, USA. **Amala Mahadevan** is Senior Scientist, WHOI, Woods Hole, MA, USA. **Julie L. McClean** is Research Oceanographer, SIO, University of California, San Diego, La Jolla, CA, USA. **Geno Pawlak** is Professor, Mechanical and Aerospace Engineering, University of California,

San Diego, La Jolla, CA, USA. **Luc Rainville** is Principal Oceanographer, APL, University of Washington, Seattle, WA, USA. **Stephen C. Riser** is Professor, School of Oceanography, University of Washington, Seattle, WA, USA. **Hyodae Seo** is Associate Scientist, WHOI, Woods Hole, MA, USA. **Andrey Y. Shcherbina** is Principal Oceanographer, APL, University of Washington, Seattle, WA, USA. **Eric Skillingstad** is Professor, College of Earth, Ocean, and Atmospheric Sciences, Oregon State University, Corvallis, OR, USA. **Janet Sprintall** is Research Oceanographer, SIO, University of California, San Diego, La Jolla, CA, USA. **Bulusu Subrahmanyam** is Professor of Satellite Oceanography and Physical Oceanography, University of South Carolina, Columbia, SC, USA. **Eric Terrill** is Director, Coastal Observing Research and Development Center, SIO, University of California, San Diego, La Jolla, CA, USA. **Robert E. Todd** is Assistant Scientist, WHOI, Woods Hole, MA, USA. **Corinne Trott** is a graduate student in the Satellite Oceanography Laboratory, University of South Carolina, Columbia, SC, USA. **Hugo N. Ulloa** is a post-doctoral researcher in the Department of Mechanical and Aerospace Engineering, University of California, San Diego, La Jolla, CA, USA. **He Wang** is a post-doctoral researcher at SIO, University of California, San Diego, La Jolla, CA, USA.

ARTICLE CITATION

Centurioni, L.R., V. Hormann, L.D. Talley, I. Arzeno, L. Beal, M. Caruso, P. Conry, R. Echols, H.J.S. Fernando, S.N. Giddings, A. Gordon, H. Graber, R.R. Harcourt, S.R. Jayne, T.G. Jensen, C.M. Lee, P.F.J. Lermusiaux, P. L'Hegaret, A.J. Lucas, A. Mahadevan, J.L. McClean, G. Pawlak, L. Rainville, S.C. Riser, H. Seo, A.Y. Shcherbina, E. Skillingstad, J. Sprintall, B. Subrahmanyam, E. Terrill, R.E. Todd, C. Trott, H.N. Ulloa, and H. Wang. 2017. Northern Arabian Sea Circulation-Autonomous Research (NASCar): A research initiative based on autonomous sensors. *Oceanography* 30(2):74–87, <https://doi.org/10.5670/oceanog.2017.224>.